MJFAS
Malaysian Journal of Fundamental and Applied Sciences

Padmaningrum *et al.* | Malaysian Journal of Fundamental and Applied Sciences, Vol. 20 (2024) 561-570

RESEARCH ARTICLE

The Complex of Cr(III) with Ligand of 2,6-Bis(pyrazol-3-yl)pyridine and Anionic Trifluoromethanesulfonate: Synthesis, Characterization and Antibacterial Activity

Regina Tutik Padmaningrum, Tuti Maryuni, Isti Yunita, Endang Widjajanti Laksono, Heru Pratomo, Kristian Handoyo Sugiyarto*

Department of Chemistry Education, Yogyakarta State University, Indonesia

Abstract The complex containing chromium(III), 2,6-bis(pyrazol-3-yl)pyridine (3-*bpp*), and $CF_3SO_3^-$ (trifluoromethanesulfonate (triflate)) has been prepared and characterized. The conductance, metal content, and *thermogravimetric and differential thermal analysis* (TGA-DTA) analysis suggest the complex to be $[Cr(3\text{-}bpp)_2](CF_3SO_3)_3{\cdot}2H_2O$. The paramagnetic moment corresponds to the three unpaired electrons being consistent with the electronic configuration of chromium(III). The electronic spectral bands are not well resolved attributed to the spin-allowed transitions of quartet ground state to quartet excited states. The IR spectral data signify the mode of vibrations typical for 3-*bpp* as well as the triflate. While the images of *scanning electron microscope-energy dispersive X-ray* (SEM) photographs confirm the crystalline particle size and the *energy dispersive X-ray* (EDX) signifies the existence of all elemental content. The analysis of powder-X-ray diffraction (powder-XRD) following the Rietica program of Le Bail suggests being a structurally orthorhombic crystal system, and *Pbca* space group, with $Z = 16$, $R_p = 4.30$, $R_{wp} = 5.14$, $R_{exp} = 12.17$, $R\text{-}F_{Bragg} = 0.04$, and *goodness of fitting (GOF)* = 0.1783. The complex shows a weak inhibition of bacterial activity against *S. aureus* and *E. coli*.

Keywords: Antibacteria, 2,6-bis(pyrazol-3-yl)pyridine, chromium(III), P-XRD, triflate.

Introduction

Studies concerning the inorganic physical properties and the powder-XRD of the divalent metal complexes such as Mn(II), Co(II), and Cu(II) in an octahedral environment of the six coordinated bidentate, bipyridine (*bipy*) and phenanthroline (*phen*), with triflate ($CF_3SO_3^-$) have been reported in detail [1-3]. Following the program of the Le Bail program to the corresponding P-XRD, it could demonstrate an acceptable refinement leading to the lattice parameters of the powder. The complex salts of *bis*-3-*bpp* with Fe(II) were studied some time ago and are currently reviewed [4], but no antibacterial aspect is involved.

Regarding the medicinal aspects, the research of metal complexes seems to involve antibacterial agent use [5-9]. A possible explanation for the toxicity of the complexes has been associated with the light of chelation theory [5].

Therefore, our research in the metal complex should extend to consider the extra role of an antibacterial agent. In this work, the two types of bacteria commonly around human life, Gram-positive and Gram-negative, will be considered, and these are *Staphylococcus aureus* and *Escherichia coli*. For those reasons, the preparation of the new powder complex containing Cr(III), the tridentate ligand of 3-*bpp*, and the triflate anion is now of interest, not only directed to the common physical inorganic properties associated with magnetism, infrared (IR), and ultraviolet-visible (UV-vis) spectral properties, P-XRD, but also to the antibacterial activity, and the results are reported.

***For correspondence:**
sugiyarto@uny.ac.id

Received: 8 Jan. 2024
Accepted: 14 April 2024

Materials and Methods

Chemical Materials

The reagents of $CrCl_3.6H_2O$ (p.a., ≥ 98.0%), $CuSO_4.5H_2O$ (ACS reagent, ≥ 98.0%), $Ca(NO_3)_2$ (ACS reagent, 99%), $Fe(NO_3)_3.9H_2O$ (ACS reagent, ≥ 98%), $Ni(NO_3)_2.6H_2O$ (p.a., ≥ 98.5%), and KCl (ACS reagent, 99.0-100.5%), for the conductivity measurement, and CF_3SO_3K (≥ 98.0%) for the anionic complex preparation were purchased from Sigma-Aldrich, and no particular treatment prior usage. Whereas, *Nutrient Agar* (NA) and *Nutrient Broth* (NB) chloramphenicol*, Staphylococcus aureus* bacteria, and *Escherichia coli* bacteria*,* for antibacterial measurement, were purchased from the Laboratory of the Department of Biology, Yogyakarta.

Preparation of 2,6-bis(pyrazol-3-yl)pyridine Ligand, 3-bpp, and the Cr(III) Complex

The ligand 2,6-bis(pyrazol-3-yl)pyridine, 3-*bpp*, (**Scheme 1**) was obtained from Sugiyarto *et al*. [10] as reported following the adapted method of Lin and Lang [11].

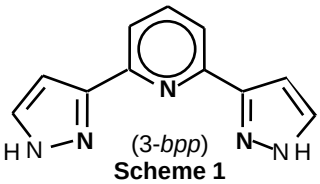

Scheme 1

The Cr(III) complex of 3-*bpp* was prepared according to the anionic replacement reaction as follows. Into an ethanolic solution of 3-*bpp* (0.259 g; 1.2 mmol, ~4 mL), an aqueous solution of $CrCl_3.6H_2O$ (0.164 g; 0.6 mmol, ~3 mL was added while warming. After filtering the mixture, an aqueous solution of CF_3SO_3K in excess (0.7 g; 3.6 mmol, ~3 mL) was added into it whereupon the yellow-orange solid produced on reducing the volume while scratching. The solid was collected by filtering, washing with minimum cold water, drying in aeration, and storing in a desiccator over P_2O_5. The preparation of the powder complex was done separately three times to confirm the reproducibility and in magnetic measurements. The complex formula is to be six N-coordinated of *bis*(3-*bpp*) to Cr(III), $[Cr(3\text{-}bpp)_2]^{2+}$.

Physical Measurements

Magnetism. The mass magnetic susceptibility (χ_g) of the complex was obtained using Magnetic Susceptibility Balance of Auto Sherwood Scientific 240V-AC calibrated with $CuSO_4{\cdot}5H_2O$ before measurement. The powder of the complex was packed tightly in the Gouy tube. The mass was recorded with and without a magnet, and the difference of the two reflected the χ_g. Following conversion into molar susceptibility (χ_M) and involving Pascal's constant [12,13] for diamagnetic correction, the corrected χ_M' is obtained to arrive at the effective magnetic moment (μ_{eff}) as for the general relationship, $\mu_{eff} = 2.83\sqrt{(\chi_M\text{'}.T)}$ BM [14-16] at the temperature T, of the sample.

Ultraviolet-visible (UV-vis) electronic and infrared (IR) spectra. The electronic spectrum of the complex was recorded in the range of 300-800 nm by using a spectrophotometer of Pharmaspec UV. The IR spectrum of the complex mixed with KBr was collected in the range of 400-4000 cm^{-1} using a spectrophotometer of the FTIR-ABB MB3000.

Metal content and ionic property. The metal content of chromium in the complex was estimated by using An AAS of the PinAAcle 900T Perkin Elmer. The ionic property of the complex was estimated using a conductometer of the Lutron CD-4301 after calibrated with an aqueous solution of 1 M KCl at 25°C before measurement, and some known ionic salts, $CrCl_3$, $CuSO_4$, $CaCl_2$, $Fe(NO_3)_3$, and $Ni(NO_3)_2$, were also recorded for comparison.

Thermogravimetric and differential thermal analysis (TG-DTG). The presence of water molecules solvated in preparing the complex was deduced from the TG-DTG data performed by a Diamond Perkin Elmer equipped with a NETZSCH STA 409C/CO thermal analyzer with the rate of 10°C/min.

Scanning electron microscope-energy dispersive X-ray (SEM-EDX). The topographic structure of complex compounds was recorded using SEM-EDX JSM-6510LA with magnifications 100x, 1000x, 5000x, and 10000x. The powdered sample was placed in a particular cell by attaching it using carbon tape. It was then introduced into the SEM-EDX tool and bombarded with electrons. The focused electron beam scanned and hit the sample resulting in issuing new electrons of the sample which are received by the detector and sent to monitors as an image pattern of the sample.

Powder-X-ray diffraction (P-XRD). A Rigaku Miniflex 600 40 kW 15 mA benchtop diffractometer with Cu*Kα*, λ = 1.5406 Å was used to record the diffractogram of the complex. The powder X-ray diffraction pattern was obtained from a benchtop diffractometer of Rigaku Miniflex 600 40 kW 15 mA with Cu*Kα*, λ

= 1.5406 Å. The scan mode within the range 2–90 degrees of 2θ in the interval of 0.04 steps per 4 sec for 2 h was applied. The corresponding diffractogram was refined by the application of the Le Bail program over the range of 10-50 degrees of 2θ in 30 cycles.

Determination of the antibacterial activity. The antibacterial activities of the complex were tested against *Staphylococcus aureus* (ATCC 25924) as Gram-positive type and *Escherichia coli* (ATCC 35218) as Gram-negative type according to agar disk-diffusion method by the media of *Nutrient Agar* (NA) and *Nutrient Broth* (NB). *Chloramphenicol* was applied as the standard antibacterial agent (positive control), while water was used as negative control. The inhibition area (in mm) of the antibacterial activities was recorded every 3 hours during 24 hours of incubation on the concentration series, 125, 250, 500, and 1000 µg/mL of the complex. Measurements were done using a caliper (accuracy 0.02 mm) on 3 sides of the sample [17, 18]. All preparation of samples in the media was done in an autoclave and the antibacterial activity test was done under Laminar flow.

Results and Discussion

Conductance, AAS, TG-DTG, and the Chemical Formula of the Complex

Direct interactions of the 3-*bpp* and chromium(III) chloride in the solution resulted in a brownish solution of the cationic complex which precipitated to an orange powder on the addition of an excessive potassium triflate salt. The ionic nature of this salt was determined by measuring the equivalent electrical conductance estimated based on several known simple compounds, and the results are listed in Table 1. The conductance of the complex falls in the range of the commonly known ionic compound containing four ions per molecule, and this suggests the stoichiometric empirical formula to be $[Cr(3\text{-}bpp)_n](CF_3SO_3)_3{\cdot}xH_2O$, where n = 2. Hence, the formula of the complex exhibits typically an uncoordinated anion of triflate, as it was also observed for the corresponding Fe(II) [19, 20].

Table 1. The equivalent electric conductance of the complex and several simple known salts in aqueous solution

Compounds	Equivalent conductance, Λc, ($\Omega^{-1}cm^2mol^{-1}$)	The ratio of the number of cations to anions	Number of ions per molecule
$CuSO_4$	84.5614	1:1	2
$CaCl_2$	160.1258	1:1	2
$CuCl_2$	172.0782	1:2	3
$Ni(NO_3)_2$	178.4155	1:2	3
$Fe(NO_3)_3.9H_2O$	285.5122	1:3	4
$CrCl_3.6H_2O$	436,8101	1:3	4
$[Cr(3\text{-}bpp)_n](CF_3SO_3)_3{\cdot}xH_2O$	**320.9851**	**1:3**	**4**

According to the thermogravimetric profile as depicted in Figure 1 and decomposition data listed in Table 2, the mass loss of about 3.715 % in the first stage, up to 50°C (*ca.* 3.762 % for $2H_2O$, giving an error of 1.17%), might strongly suggest being the loss of water molecule [21]. Considering the metal content of Cr, obtained from AAS data of 6.19 % (*ca.* 5.43 %, giving an error of 12.27%), this is likely to suggest confirming the proposed stoichiometric formula of the complex to be $[Cr(3\text{-}bpp)_2](CF_3SO_3)_3{\cdot}2H_2O$.

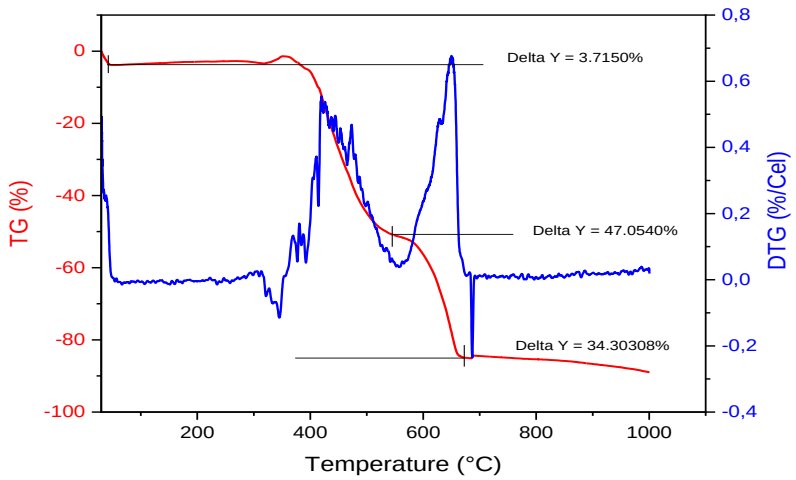

Figure 1. The TG-DTG thermogram of $[Cr(3\text{-}bpp)_2](CF_3SO_3)_3{\cdot}2H_2O$ at 30-1000°C

Table 2. The proposed formula of the complex due to the hydrate and metal content estimated by TG-DTG and AAS data showing the percentage of calculated error figures (in brackets*)

Proposed complex	H_2O content (%)		Cr content (%)	
	calculated	TGA-DTG	*calculated*	AAS
$[Cr(3\text{-}bpp)_2](CF_3SO_3)_3{\cdot}1H_2O$	1.915 (48.45*)		5.53 (10.66*)	
$[Cr(3\text{-}bpp)_2](CF_3SO_3)_3{\cdot}2H_2O$	**3.762** (1.86*)	**3.715**	**5.437** (12.27*)	**6.19**
$[Cr(3\text{-}bpp)_2](CF_3SO_3)_3{\cdot}3H_2O$	5.53 (32.82*)		5.33 (13.89*)	

Although the thermographic profile (Figure 1) seems well to contain only three simple stages of weight loss, it is not easy to explain the corresponding compound as confirmed in Table 3. Each stage does not reflect the complete loss of a specific compound, but rather an unclear mixture. The loss of the first stage (up to 50°C) might be fixed for dehydration, but the next two stages (50-520°C and 520-680°C) and the residue seem uncertain species. The second-third stage loss (81.357%) is mostly due to 2 molecules of 3-*bpp*, two molecules of triflate, and a "radical" CF_3, which are calculated at about 87.887%. The remaining (14.571%) is likely believed to be the slow conversion of metal-SO_3 (cal. 12.102%) to metal-metal oxide(s) by assuming the decomposition is not finished yet at the experimental temperature (1000^0C). It should be noted that while the absence of the mass-spectroscopic data, this analysis is not confirmed.

Table 3. TG-DTA data of $[Cr(3\text{-}bpp)_2](CF_3SO_3)_3{\cdot}2H_2O$

Lost of Weight	TG-DTA (%)	Calculated (%)	Species
First stage	**3.715**	**3.762**	**$2H_2O$**
Second stage	47.054	44.111	2(3-*bpp*)
Third stage	34.303	31.131	$2(CF_3SO_3)$
		8.883	CF_3
1^{st} - 3^{rd} stages	**85.429**	**87.887**	
The rest	**14.571**	**6.683**	SO_3
		5.429	Cr

Magnetism

For the magnetic susceptibility measurement, the three samples of the Cr(III) complex were prepared separately to confirm the reproducibility. The magnetic data as listed in Table 4, produce the moments of 3.7- 4.1 BM, being comparable to the other reported data of various Cr(III) complexes, which are to be 3.51-4.19 BM [22], 3.77-3.84 BM [23], and 3.71-3.84 BM [24]. The moments are very close to the value of spin only, μ_s, for the 3 unpaired electrons (3.87 BM) in the $3d^3$ configuration of Cr(III), and therefore, there is no orbital contribution to the magnetic moment was observed as predicted by the single degeneracy [13-16].

Table 4. Magnetic moment of $[Cr(3\text{-}bpp)_2](CF_3SO_3)_3{\cdot}2H_2O$

Sample	T (K)	χ_g (cgs)	μ_{eff} (BM)
1	291	8.61084 x10^{-6}	4.182
2	291	6.98844 x10^{-6}	3.743
3	291	7.17792 x10^{-6}	3.797

Electronic Spectrum

Figure 2 shows the two UV-vis spectra of the complex recorded as powder and in solution. The slightly similar pattern of the two suggests being stability of the complex in both states. The spin only of magnetic data of octahedral Cr(III) in the complex suggests having no triply ground state of the quartet, but $^4A_{2g}$ (single degeneracy). Therefore, following the Tanabe-Sugano diagram [13] for the ideal octahedral geometry, the three possible spin-allowed transitions, $^4A_{2g}(F) \rightarrow {}^4T_{2g}(F)$, $^4A_{2g}(F) \rightarrow {}^4T_{1g}(F)$, and $^4A_{2g}(F) \rightarrow {}^4T_{1g}(P)$, might assign to the main electronic spectrum of the complex. The spectra of the complexes under study show bands below 30000 cm^{-1} [25] and the extinction coefficient (Figure 2) is too high which cannot be interpreted in terms of idealized O_h symmetry.

As depicted in Figure 2, however, the spectra are not well resolved and exhibit only an indicative of the spin-allowed transitions, the first broad ligand field band centered at ~19500 cm^{-1} (ν_1), the second shoulder at ~20500 cm^{-1} (ν_2), the third shoulder at ~22000 cm^{-1} (ν_3), and the forth at ~ 23000 cm^{-1} (ν_4). By assuming in a lower symmetry of D_{4h}, those bands are comparable to the complex of $[Cr(terpy)_2]^{3+}$ reported (using Gaussian/Loretzian analysis) by Sulekh Chandra & Poonam Pipil, 2014 [24], and thus, in the present complex the four bands observed might be attributed to the $^4B_{1g} \rightarrow {}^4E_{ag}$ (ν_1), $^4B_{1g} \rightarrow {}^4B_{2g}$ (ν_2), $^4B_{1g} \rightarrow {}^4E_{bg}$ (ν_3) and $^4B_{1g} \rightarrow {}^4A_{a1g}$ (ν_4) transitions respectively, reflecting a singe degeneracy ground term.

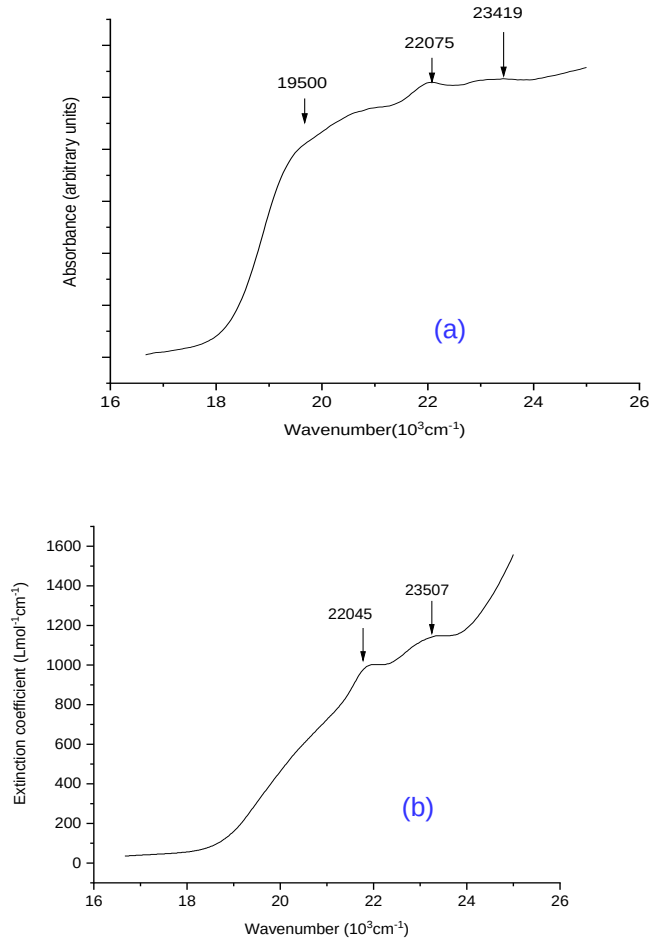

Figure 2. Electronic spectra of $[Cr(3\text{-}bpp)_2](CF_3SO_3)_3.2H_2O$: powder (a), and in aqueous solution, 0.005 M (b)

Infrared Spectra

The IR spectrum of the complex, $[Cr(3\text{-}bpp)_2](CF_3SO_3)_3.2H_2O$, is displayed in Figure 3, together with that of CF_3SO_3K, thus allowing the direct assignment. The broadband (Figure 3A-red full line) at about 3399 cm^{-1} is likely due to the stretching modes of -OH of the H_2O, being symmetric-/anti symmetric- lattice as strongly indicated in the first stage loss in the TG-DTA graph (Figure 1) for the complex. This is comparable as observed by Abebe, Kendie, & Tigineh, 2022, at 3398 cm^{-1} [26], by Shad *et al.*, 2011, at around 3441 cm^{-1} [27], even though Kumar *et al.*, 2014, reported that to be an aromatic of C-C at around 3430 cm^{-1} [28]. The band centered at about 3434.87 cm^{-1} is associated with the stretching mode of O-H in H_2O as observed by Ma, *et.al*., 2021, at 3475−3412 cm^{-1} [29] and Pervaiz, *et.al.*, 2020, at 3400-3500 cm^{-1} [30].

The stretching modes at 3141-2750 cm^{-1} are likely to the NH and CH stretching region of the IR spectrum of the pyrazole ring being comparable as observed by Rice *et al.*, 2005 [31], and Rastegarnia, *et al.,* 2019 [32]. While the three sharp modes at the region 1620-1450 cm^{-1} and at about 760 cm^{-1} are likely attributed to the ν(C=C) stretching, ν(C=C-N) stretching, ν(N-H) bending, and ν(C-H) stretching of pyridine in 3-*bpp* as being comparable with those reported by Gamez *et al.*, 2002 [33] for free 3-*bpp* of Cu(II).

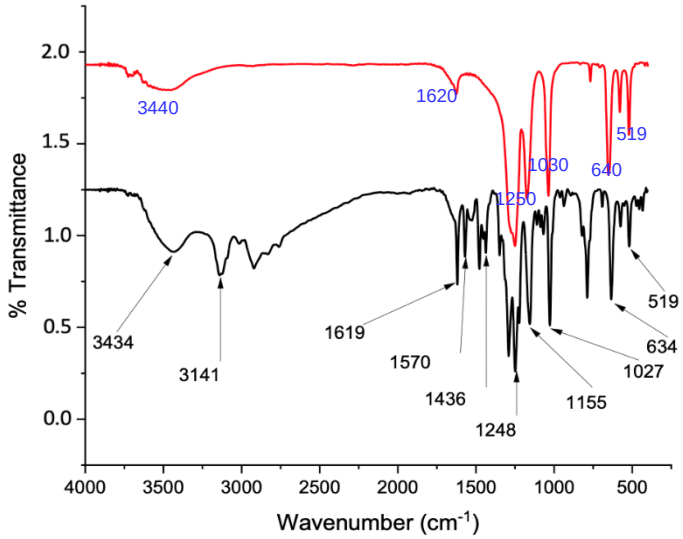

Figure 3. IR Spectra of $[Cr(3\text{-}bpp)_2](CF_3SO_3)_3.2H_2O$ (black) and CF_3SO_3K. $4H_2O$ (red) with numbering of selected peaks indicated

SEM, EDX, and Powder-XRD

Particle size as indicated in the image of SEM, Figure 4 (a), might consider the powder complex to be relatively bulky polycrystalline rather than amorphous type. The EDX profile (Figure 4*b*) confirms the presence of all elemental content (Cr, N, C, F, and S) except for hydrogen.

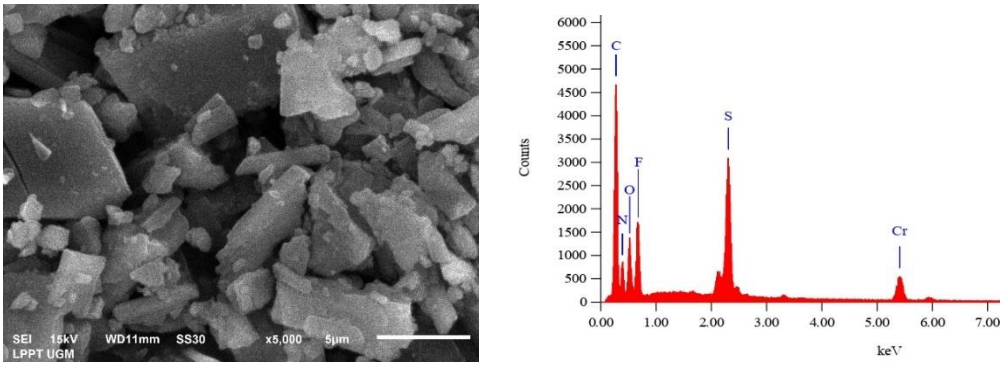

(a) (b)

Figure 4. SEM photograph of $[Cr(3\text{-}bpp)_2](CF_3SO_3)_3.2H_2O$ at a magnification of 10000 times showing crystalline solid (*a*) and EDX showing elemental content (b)

The lattice parameters of the powder $[Cr(3\text{-}bpp)_2](CF_3SO_3)_3.2H_2O$ were deduced from the results of the refinement of the diffractogram following the Le Bail program, and it is described in Figure 5 and Table 5. For comparison, the cell parameters of a single crystal of $[Cr(tpy)_2]^{3+}$ [34] were listed.

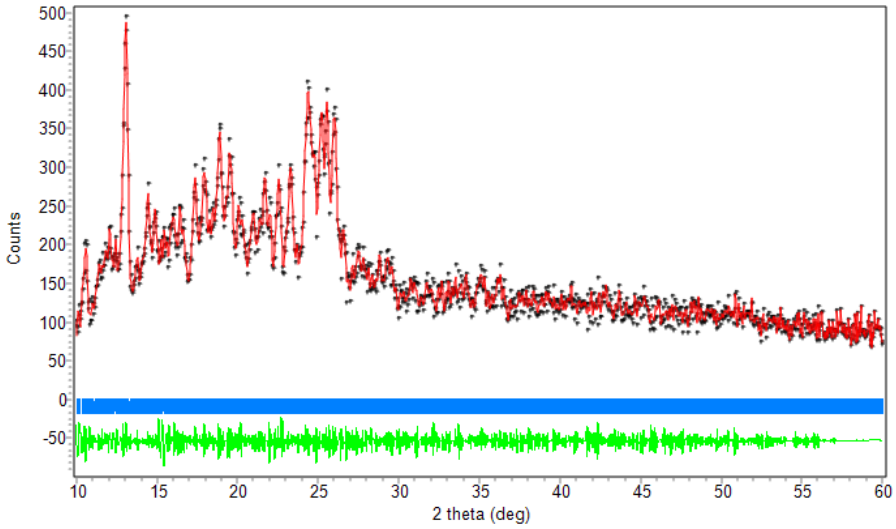

Figure 5. P-XRD profile of $[Cr(3\text{-}bpp)_2](CF_3SO_3)_3.2H_2O$ (black), the refinement on orthorombic symmetry of *Pbca* (red), the position of 2θ (blue), and the difference in intensity (green) between the experimental data (black) and the refinement lines (red) showing almost flat.

Table 5. Lattice parameter data of $[Cr(3\text{-}bpp)_2](CF_3SO_3)_3.2H_2O$

Complex Compound	$[Cr(3\text{-}bpp)_2](CF_3SO_3)_3.\ 2H_2O$	$2\{[Cr(tpy)_2][PF_6]_3\}.\ 5MeCN$[*)]
Crystal System	Orthorombic	Orthorombic
Space group	*Pbca*	*Pbca*
a (Å)	21.9853	22.0190(11)
b (Å)	32.5696	32.5520(17)
c (Å)	47.3629	47.334(3)
α (°)	90	90
β (°)	90	90
γ (°)	90	90
V(Å^3)	33914	33927
Z	16	16
The Figure of Merits		
R_{exp}	12.17	-
R_p	4.3	-
R_{wp}	5.14	-
Gof	0.1783	1.056
$R\text{-}F_{Bragg}$	0.04	-

[*)]Constable, *et al.,* 2014 [34].

As shown in Figure 5, the red line of the refinement passes through almost all the black points of experimental XRD data at the blue bars space group and symmetry model. The distribution of the green line demonstrating the difference between the original experimental data and the refinement model seems to be flat-linear. In addition, the figure of merits is to be acceptable low. For these reasons, the refinement should satisfy the model, and hence it can be concluded that the powdered complex adopts a space group of *Pbca*, with cell parameters of, a = 21.9853 Å, b = 32.5696 Å, c = 47.3629 Å, α = 90°, β = 90°, γ = 90°, V = 33914 Å^3. The figure merits of R_{exp} = 12.17, R_P = 4.30, R_{WP} = 5.14, $R\text{-}F_{Bragg}$ = 0.04, and *goodness of fitting* (GOF) = 0.1783, the refinement might be acceptable.

Antibacterial Activity Test

The medicinal aspect of the complex was tested against the activity of *Staphylococcus Aureus* (*S.A*) and *Escherichia Coli* (*E.C*) bacteria. They represent the two types, Gram-positive and Gram-negative,

respectively, which are pathogenic and easily found in humans. In this, *chloramphenicol* was applied as a positive control following the agar disc-diffusion method in *Nutrient Agar* (NA) and *Nutrient Broth* (NB) or diffusion assay procedures [18,35]. All numerical data of the diameter of the clear inhibition zone (in mm) with time (in hours) to the concentration of the complex are summarized and displayed in Figure 6 and Figure 7.

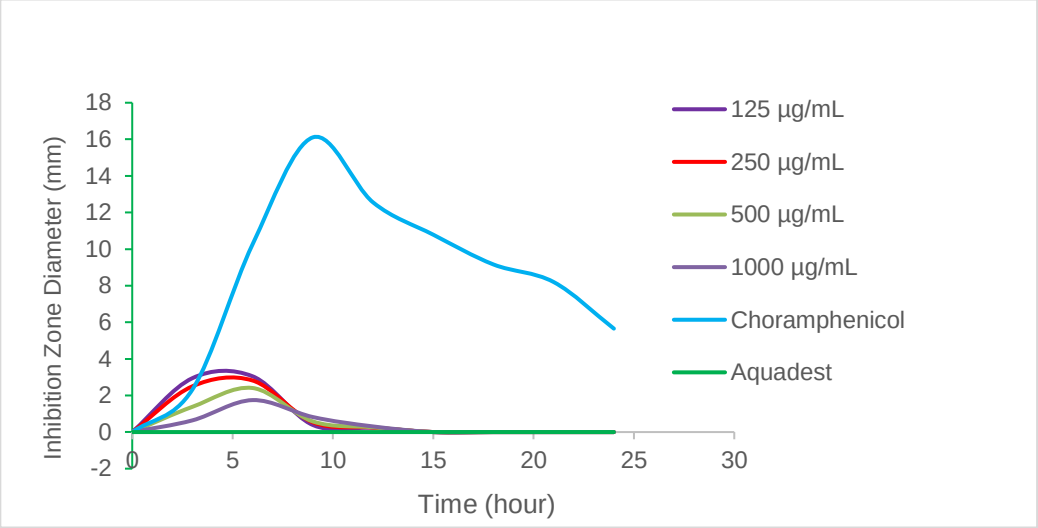

Figure 6. Graph of the clear inhibition zone diameter (in mm) with concentrations of the complex, [Cr(3-*bpp)*$_2$](CF_3SO_3)$_3$.2H_2O, against the time of *S. aureus* activity

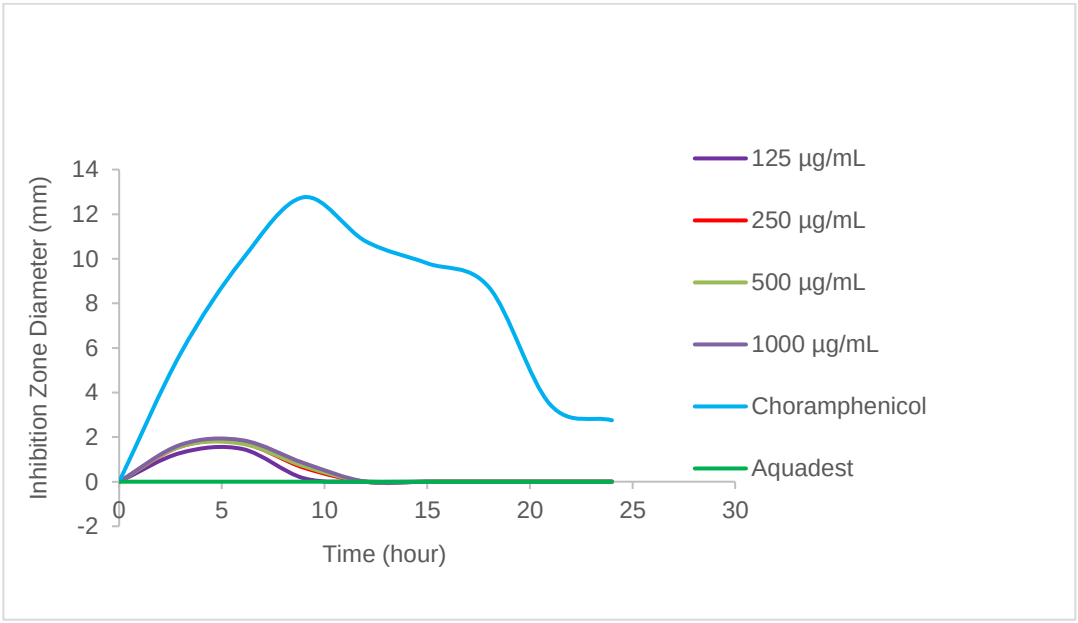

Figure 7. Graph of the clear inhibition zone diameter (in mm) with concentrations of the complex, [Cr(3-bpp)$_2$](CF_3SO_3)$_3$.2H_2O, against the time of *E. coli* activity

Following the *Kolmogorov-Smirnov* test, it was found that the diameter data of the clear inhibition zone is not normally distributed ($p = 0.000$; $p < 0.05$), and then by *Levene's test,* it is found to be inhomogeneous data ($p = 0.000$; $p < 0.05$). By the next non-parametric test, *Kruskal-Wallis* and *Mann-Whitney test*, it can be concluded that the complex in all variant concentrations falls statistically into no different category ($p = 0.000$; $p < 0.05$), and being a weak antibacterial agent [35]. Table 6 shows the average inhibition zone of the complex at the optimum time of six hours and that of the positive-negative control, *chloramphenicol-aquadest*, at nine hours.

Table 6. The average inhibition zone diameter with concentration of the complex and the antibacterial power

Concentration of the complex	The average inhibition zone diameter (mm)		Category of antibacterial power
	Due to *S. aureus*	Due to *E.coli*	
125 µg/mL	0.82667	0.36417	weak
250 µg/mL	0.76208	0.4925	weak
500 µg/mL	0.57833	0.49667	weak
1000 µg/mL	0.43917	0.54417	weak
Aquadest	0	0	none
Chloramphenicol	9.3475	8.3025	strong

In the light of chelation theory, the *bipy* ligand may be considered to be highly stable, however, the high-spin complex of Cr(III) suggests that the tris-ligand provides significantly a weak ligand field strength, and this might cause a weak antibacterial agent, as quite recently observed for $[Mn(bipy)_3](CF_3SO_3)_2$ [3].

Conclusions

The complex of $[Cr(3\text{-}bpp)_2](CF_3SO_3)_3.2H_2O$, has been successfully prepared and confirmed by the physical properties. The corresponding lattice parameters have been estimated following Le-Bail refinement to the P-XRD diffractogram. The complex shows only a weak category in inhibiting the growth of *S. aureus* and *E. coli* bacterial activity.

Conflicts of Interest

There is no conflict of interest to declare.

Acknowledgment

Authors greatly acknowledge to the Yogyakarta State of University due to the financial support.

References

[1] Kusumawardani, C., Kainastiti, F., & Sugiyarto, K. H. (2018). Structural Analysis of Powder Complex of $Cu(bipy)_3(CF_3SO_3)_2$ $(H_2O)_x$ (x = 0.5, 1). *Chiang Mai Journal of Science*, *45* (4), 1944-1952. http://epg.science.cmu.ac.th/ejournal/

[2] Sugiyarto, K. H., Kusumawardani, C., & Wulandari, K. E. (2018). Synthesis and structural analysis of powder complex of tris(bipyridine)cobalt(ii) trifluoromethanesulfonate octahydrate, *Indonesian Journal of Chemistry*, *18* (4), 696-701. DOI: 10.22146/ijc.26833

[3] Sugiyarto, K. H., Marini, D. W., Sutrisno, H., Purwaningsih, D., & Kusumawardani, C. (2023). Synthesis of powdered $[Mn(bipy)_3](CF_3SO_3)_2 \cdot 5.5H_2O$: the physical properties and antibacterial activity. *Indonesian Journal of Chemistry, 23* (1), 242 – 250. DOI: 10.22146/ijc.77565

[4] Sugiyarto, K. H. (2019), Spin state transition in iron(II): a review on bis-[(2,6-bis(pyrazol-3-yl)pyridine]iron(II) complex, *J. Phys.: Conf. Ser.* 1156 012007. DOI:10.1088/1742-6596/1156/1/012007

[5] Singh, B. K., Mishra, P., Prakash, A., & Bhojak, N. (2017). Spectroscopic, electrochemical and biological studies of the metal complexes of the Schiff base derived from pyrrole-2-carbaldehyde and ethylenediamine, *Arabic Journal of Chemistry*, *10*(2), S472-S483. http://dx.doi.org/10.1016/j.arabjc.2012.10.007

[6] Uddin, S., Hossain, Md. S., Latif, Md. A., Karim, Md. R., Mohapatra, R. K., & Zahan, Md. K-E. (2019). Antimicrobial activity of Mn complexes incorporating schiff bases: a short review. *American Journal of Heterocyclic Chemistry, 5*(2), 27-36. DOI: 10.11648/j.ajhc.20190502.12

[7] Ayipo, Y. O., Osunniran, W. A., Badeggi, U. M., Saheed, I. O., Jimoh. A. A., Babamale, H. F., & Olaide, E. O., (2021). Synthesis, characterization and antibacterial study of Co(II) and Cu(II) complexes of mixed ligands of piperaquine and diclofenac. JOTCSA, *Journal of the Turkish Chemical Society Chemistry*, *8* (2):633–50. https://doi.org/ 10.18596/jotcsa. 898523S

[8] Beyene, B. B., & Wassie, G. A. (2020). Antibacterial activity of Cu(II) and Co(II) porphyrins: role of ligand modification. *BMC Chemistry 14*, 51:1-8 https://doi.org/10.1186/s13065-020-00701-6

[9] Sondavid, N., Shweta, B., Bryan, W., Joung, C., Naresh, T., & Jun, K. H. (2020). Cobalt(II) benzazole derivative complexes: synthesis, characterization, antibacterial and synergistic activity. *ChemistrySelect, 5*, 3471-3476. DOI:10.1002/slct.202000222

[10] Sugiyarto, K. H., Onggo, D., Hiroki Akutsu, H., Varimalla Raghavendra Reddy, V. R., Hari Sutrisno, H., Nakazawac, Y., & Bhattacharjee, A., 2021, Structural, magnetic and Mössbauer spectroscopic studies of the $[Fe(3\text{-}bpp)_2](CF_3COO)_2$ complex: role of crystal packing leading to an incomplete Fe(II) high spin ⇋ low spin transition, *CrystEngComm*, *23*, 2854- 2861. DOI: 10.1039/d0ce01687j

[11] Lin, Y-i & Lang Jr., S. A. (1977). Novel two step synthesis of pyrazoles and isoxazoles from aryl methyl ketones. *Journal of Heterocyclic Chemistry, 14* (2), 345–347. DOI:10.1002/jhet.5570140240

[12] Bain, G. A., & Berry, J. F. (2008). Diamagnetic Corrections and Pascal's Constants. *Journal of Chemical Education, 85*(4): 532-536. DOI:10.1021/ed085p532

[13] Dalal, M. A. (2017). Textbook of Inorganic Chemistry-Volume 1 (First Edition). CHAPTER 9. *Magnetic Properties of Transition Metal Complexes.* India: Dalal Institute, pp.342-386

[14] Pathshala (2021). *Inorganic Chemistry-II: Metal-Ligand Bonding, Electronic Spectra and Magnetic Properties of Transition Metal Complexes*. http://meerutcollege.org/mcm_admin/upload/1588000002.pdf). [accessed 15 December 2021]

[15] LibreTexts™ (2020). *Magnetism*. https://chem.libretexts.org/@go/page/263246). [accessed 15 December 2021]

[16] Lancashire, R. J. *LibreTexts™* (2020). *Magnetic Moments of Transition Metals*. https://chem.libretexts.org/@go/page/19707 [accessed 15 December 2021]

[17] Kani, I., Atlier, Ö., & Güven, K. (2016). Mn(II) complexes with bipyridine, phenanthroline and benzoic acid:Biological and catalase-like activity. *Journal of Chemical Sciences, 128* (4), 523–536. DOI: 10.1007/s12039-016-1050-z

[18] Balouiri, M., Sadiki, M., & Ibnsouda, S. K. (2016). Methods for in vitro evaluating antimicrobial activity: A review. *Journal of Pharmaceutical Analysis*, *6* (2), 71–79. https://doi.org/10.1016/j.jpha.2015.11.005

[19] Buchen , T., Gütlich, P., Sugiyarto, K. H., & H. A. Goodwin, H. A. (1996), High-spin → low-spin relaxation in $[Fe(bpp)_2](CF_3SO_3)_2{\cdot}H_2O$ after LEISST and thermal spin-trapping-dynamics of spin transition versus dynamics of phase transition. *Chemistry: A European Journal*. *2* (9), 1134-1138. https://doi.org/10.1002/chem.19960020915

[20] Sugiyarto, K. H., Weitzner, K., Craig, D. C., & Goodwin, H. A. (1997). Structural, magnetic and Mössbauer studies of bis(2,6-bis(pyrazol-3-yl)pyridine)iron(II) triflate and its hydrates. *Australian Journal of Chemistry*, 50(9), 869-873. DOI:10.1071/c96206

[21] Paswan, S., Anjum, A., Singh, A. P., & Dubey, R. K. (2019). Synthesis and Spectroscopic Characterization of Lanthanide Complexes Derived from 9,10-Phenanthrenequinone And Schiff Base Ligands Containing N, O Donor Atoms. *Indian Journal of Chemistry, 58A*(4), 446-453

[22] Aranha, P. E., dos Santos, M. P., Romera, S., & Dockal, E. R. (2007). Synthesis, characterization, and spectroscopic studies of tetradentate Schiff base chromium(III) complexes. *Polyhedron, 26* (7), 1373–1382. DOI:10.1016/j.poly.2006.11.005

[23] Mahmoud, M. A., Zaitone, S. A., Ammar, A. M., & Sallam, S. A. (2016). Synthesis, structure and antidiabetic activity of chromium(III) complexes of metformin Schiff-bases. *Journal of Molecular Structure*, *1108*, 60–70. DOI: 10.1016/j.molstruc.2015.11.055

[24] Sulekh, C., & Poonam, P. (2014), Chromium(lll) complexes: synthesis, spectral characterization and microbial studies, *Journal of Chemical and Pharmaceutical Research*, 2014, *6* (6):44-54

[25] Sinha, N., Jiménez, J-M., Pfund, B., Prescimone, A., Piguet, C., & Wenger, O. S. (2021). A near-infrared-II emissive chromium(III) complex. *Angewandte Chemie International Edition, 60,* 23722–23728. DOI:10.1002/anie.202106398

[26] Abebe, A., Kendie, M., & Tigineh, G.T. (2022). Mono-and Binuclear Cobalt(II) Mixed Ligand Complexes of 2,2'-Bipyridine and Ethylenediamine: Synthesis, Characterization and Biological Application. *Biointerface Research in Applied Chemistry, 12,* 1962-1973. https://doi.org/10.33263/BRIAC122.19621973

[27] Shad, H. A., Thebo, K. H., Ibupoto, Z. H., Malik, M. A., O'Brien, P., & Raftery, J. (2011). Synthesis, characterization, and crystal structure of a copper(II) complex of 1,10-phenanthroline and succinate, *Journal of Coordination Chemistry*, *64*(13), 2353-2360. DOI: 10.1080/00958972.2011.595789

[28] Kumar, S. P., Suresh, R., Giribabu, K., Manigandan, R., Munusamy, S., Muthamizh, S., & Narayanan, V. (2014). Microwave synthesis of Tris-(1,10-phenanthroline)Manganese(II) complex and its electrochemical sensing property of catechol. *International Journal of ChemTech Research*, *6* (6), 3280-3283

[29] Ma, X., Jing, J., Yu, J., Wang, J., Zhu, H., & Hu, Z. (2021). Synthesis and Characterization of a Novel Apple Pectin–Fe(III) Complex. *ACS Omega, 6* (2), 1391–1399. DOI:10.1021/acsomega.0c05029

[30] Pervaiz, M., Riaz, A., Munir, A., Saeed, Z., Hussain, S., Rashid, A., & Adnan, A. (2019). Synthesis and characterization of sulfonamide metal complexes as antimicrobial agents. *Journal of Molecular Structure, 1202*(10):127284. DOI:10.1016/j.molstruc.2019.127284

[31] Rice, C. A., Borho, N., & Suhm, M. A. (2005). Dimerization of Pyrazole in Slit Jet Expansions. *Zeitschrift für Physikalische Chemie, 219(3-2005), 379–388.* doi:10.1524/zpch.219.3.379.59183)

[32] Rastegarnia, S., Pordel, M., & Allameh, S. (2020). Synthesis, characterization, quantum-chemical investigation and antibacterial studies of new fluorescent Cr(III) complexes. *Arabian Journal of Chemistry*. *13, 3903-3909.* DOI:10.1016/J.ARABJC.2019.03.001

[33] Gamez, P., Steensma, R. H., Driessen, W. L., & Reedijk, J. (2002). Copper(II) compounds of the planar-tridentate ligand 2,6-bis(pyrazol-3-yl)pyridine. *Inorganica Chimica Acta*, *333* (1), 51–56. DOI:10.1016/s0020-1693(02)00754-5

[34] Constable, E. C., Housecroft, C. E., Neuburger, M., Schönle, J., & Zampese, J. A. (2014). The surprising lability of bis(2,2′:6′,2″-terpyridine)chromium(III) complexes. *Dalton Trans*., *43* (19), 7227–7235

[35] Davis, W. W., & Stout, T. R. (1971). Disc plate method of microbiological antibiotic assay. I. Factors influencing variability and error. *Applied Microbiology*, *22*(4), 659-65. DOI: 10.1128/am.22.4.659-665.1971. PMID: 5002143; PMCID: PMC376382.